Mathematical Analysis of Stochastic Perturbations in Astrocytic Metabolic Dynamics

Bingyu JIANG

1 Introduction

The brain's remarkable computational power relies on a partnership between two cell types: neurons, which transmit electrical signals, and astrocytes, which provide metabolic support. This relationship operates through an intricate biochemical conversation where calcium ions—charged particles that serve as cellular messengers—coordinate energy production with neural activity. Understanding how this communication system responds to random molecular fluctuations reveals fundamental principles about biological robustness and cellular homeostasis.

This investigation explores how different patterns of molecular noise influence a critical calcium pathway in astrocytes and examines whether these perturbations affect downstream energy metabolism. The experimental framework builds on the astrocyte-neuron lactate shuttle hypothesis, which proposes that astrocytes convert glucose into lactate (a metabolic fuel) and deliver it to neurons based on calcium-mediated signals from an internal storage compartment called the endoplasmic reticulum (ER), as illustrated in Figure 1.

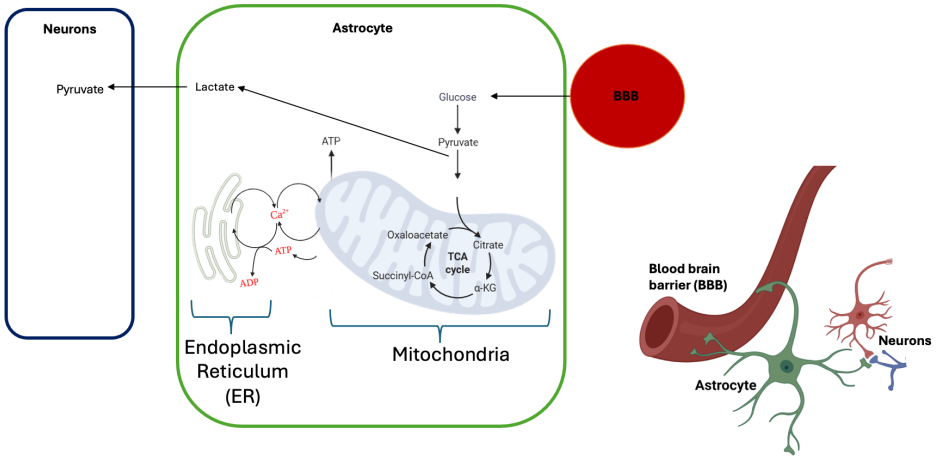

Figure 1: Schematic representation of astrocyte-neuron metabolic coupling. The blood-brain barrier (BBB) supplies glucose to astrocytes, which convert it to pyruvate through glycolysis and lactate via lactate dehydrogenase. Lactate is then shuttled to neurons for oxidative metabolism. The process is regulated by calcium signaling through IP3 receptors in the endoplasmic reticulum.

To understand the biological machinery at work, consider that cells maintain distinct chemical environments in different compartments. The endoplasmic reticulum acts as

a calcium warehouse, storing high concentrations of calcium ions that can be rapidly released into the main cellular space (the cytosol) when needed. This release occurs through specialized protein channels called IP3 receptors, which open in response to a signaling molecule called inositol trisphosphate (IP3). When these channels open, calcium floods into the cytosol, triggering a cascade of metabolic responses that ultimately increase ATP production—the universal energy currency of cells.

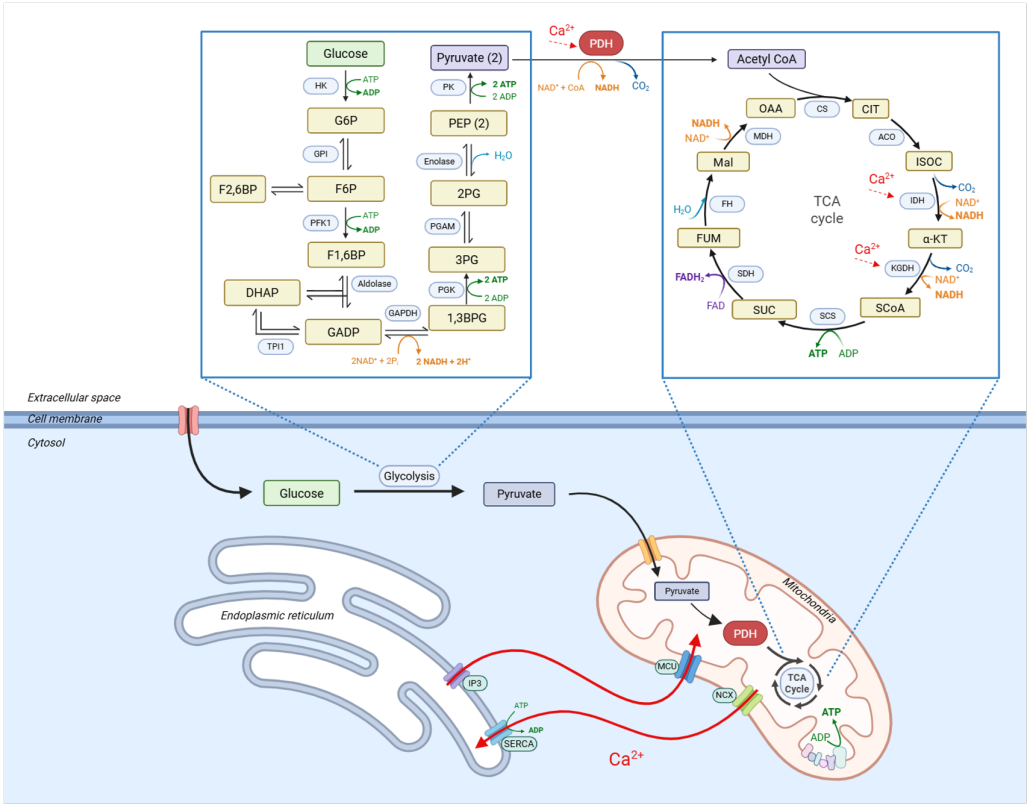

Figure 2: Detailed biochemical pathways in astrocyte glucose metabolism. Left panel shows glycolysis with key intermediates. Right panel depicts the TCA cycle and its connection to calcium signaling through mitochondrial metabolism. Calcium release from the ER is coupled to ATP production via the SERCA pump and metabolic enzyme activation.

The system operates through negative feedback: calcium release from the ER depletes its stores, triggering energy-consuming pumps (SERCA pumps) to reload the ER with calcium. This creates oscillations—rhythmic rises and falls in calcium and ATP levels, which are not merely curious mathematical patterns but appear to optimize metabolic efficiency by synchronizing calcium signals with mitochondrial ATP production cycles.

2 Theoretical Framework

2.1 Research Objective

The central question driving this study is both fundamental and practical: *How do different forms of random molecular fluctuations applied to calcium release channels propagate through the cell's metabolic network?* More specifically, we investigate whether the

mathematical character of noise—its amplitude scaling properties and temporal correlations—determines how effectively it disrupts cellular function. We also identify which cellular compartments act as shock absorbers versus which transmit variability to downstream processes.

This question matters because all biological systems operate under constant molecular bombardment. Ion channels open and close stochastically due to thermal fluctuations, enzyme reactions occur randomly rather than smoothly, and diffusing molecules arrive at their targets following probabilistic rather than deterministic trajectories. Evolution has shaped biological systems to function reliably despite this intrinsic randomness, but the mechanisms underlying this robustness remain poorly understood.

2.2 Deterministic Model

Before introducing randomness, we must establish the deterministic foundation. The mathematical model describes 30 interconnected metabolites whose concentrations change according to reaction rates and transport processes. At the heart of this system lie three calcium fluxes that determine the calcium concentration in two compartments.

The mathematical description of calcium dynamics captures these processes through differential equations:

$$\frac{d[\mathrm{Ca}^{2+}]_c}{dt} = \mu_M f_c \left(-J_{\mathrm{SERCA}} + J_{\mathrm{ER,out}} + \delta(J_{\mathrm{NCX}} - J_{\mathrm{uni}})\right)$$
$$\frac{d[\mathrm{Ca}^{2+}]_{\mathrm{ER}}}{dt} = \mu_M \delta_{\mathrm{ER}} \left(J_{\mathrm{SERCA}} - J_{\mathrm{ER,out}}\right)$$

Here, square brackets denote concentrations, subscript c indicates cytosol, subscript ER indicates endoplasmic reticulum, and J terms represent flux rates (amount of calcium moving per unit time). The IP3 receptor flux $J_{\mathrm{ER,out}}$ has a complex functional form reflecting the channel's regulation by three factors:

$$J_{\mathrm{ER,out}} = \left[\left(v_{\mathrm{IP3}} \frac{[\mathrm{IP3}]^2}{[\mathrm{IP3}]^2 + K_{\mathrm{IP3}}^2} \frac{[\mathrm{Ca}^{2+}]_c^2}{[\mathrm{Ca}^{2+}]_c^2 + K_{\mathrm{act}}^2} \frac{K_{\mathrm{inh}}^4}{K_{\mathrm{inh}}^4 + [\mathrm{Ca}^{2+}]_c^4}\right) + v_{\mathrm{leak}}\right] \frac{[\mathrm{Ca}^{2+}]_{\mathrm{ER}} - [\mathrm{Ca}^{2+}]_c}{\mu_M}$$

This equation encodes three regulatory mechanisms: IP3 binding activates the channel (first fraction), low cytosolic calcium activates the channel further (second fraction), but high cytosolic calcium inhibits it (third fraction). This biphasic calcium dependence—activation at low levels, inhibition at high levels—creates the oscillatory behavior. The model also includes a small constant leak term representing basal calcium permeability.

The existing mathematical framework, developed by Voorsluijs et al. (2024), implements these dynamics through a system of 17 coupled ordinary differential equations (ODEs) in Python, capturing not only calcium dynamics but also glycolytic intermediates, mitochondrial metabolism, and ATP/ADP cycling, as shown in Figure 3. The latest version of this system is extended to 30 equations to incorporate additional metabolic pathways relevant to astrocyte function.

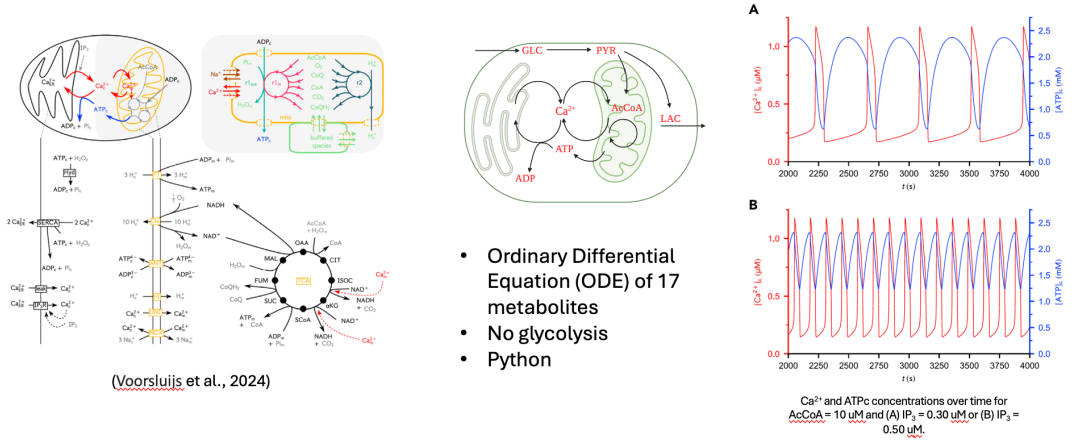

Figure 3: Existing ODE model framework. Left: Comprehensive interaction network showing calcium dynamics, mitochondrial metabolism, and glycolytic pathways. Center: Simplified schematic of astrocyte calcium-ATP coupling via IP3 receptors and mitochondria. Right: Model predictions showing oscillations in Ca^{2+} and ATP concentrations under different conditions (A: $IP_3 = 0.30$ μM, B: $IP_3 = 0.50$ μM). The model captures the fundamental 100-second period oscillations observed experimentally.

2.3 Stochastic Perturbation Schemes

Real biological systems never follow deterministic trajectories because molecular events are inherently random. Ion channels flicker open and closed stochastically, the number of active channels fluctuates due to random activation and deactivation events, and local calcium concentrations vary due to diffusion-limited transport. To investigate how these different forms of randomness affect cellular function, we introduce five mathematically distinct noise paradigms applied to the IP3 receptor calcium flux.

The critical question is whether the mathematical form of noise matters for biological function. Does the system respond differently to noise that has constant amplitude regardless of system state (additive) versus noise whose amplitude scales with the flux magnitude (multiplicative)? Do temporal correlations in the noise—situations where random fluctuations at one moment influence fluctuations at nearby moments—penetrate cellular defenses more effectively than uncorrelated white noise? Can abrupt, intermittent perturbations disrupt function more than continuous diffusion? We hypothesize that homeostatic mechanisms may buffer against noise regardless of its mathematical form, but that certain temporal structures may exploit resonance effects to penetrate more deeply into metabolic dynamics.

2.3.1 Additive Gaussian Noise

Additive noise represents external perturbations whose magnitude is independent of the system's current state. Imagine random fluctuations in membrane potential or stochastic arrival of signaling molecules that perturb calcium release regardless of whether the flux is currently high or low. Mathematically, this is captured through an Itô stochastic differential equation:

$$dX_t = f(X_t, t)dt + \sigma_{\text{add}} dW_t$$

The term dW_t represents a Wiener process (mathematical Brownian motion), and $\sigma_{\text{add}} = 5$ quantifies the noise intensity with units matching the flux. In our calcium

system, this adds a constant-amplitude random perturbation to both ER and cytosolic calcium:

$$d[\mathrm{Ca}^{2+}]_{\mathrm{ER}} = \mu_M \delta_{\mathrm{ER}}(J_{\mathrm{SERCA}} - J_{\mathrm{ER,out}})dt - \sigma_{\mathrm{add}}\mu_M \delta_{\mathrm{ER}} dW_t$$
$$d[\mathrm{Ca}^{2+}]_c = \mu_M f_c(-J_{\mathrm{SERCA}} + J_{\mathrm{ER,out}} + \delta(J_{\mathrm{NCX}} - J_{\mathrm{uni}}))dt + \sigma_{\mathrm{add}} f_c \delta_{\mathrm{ER}} dW_t$$

Note the opposite signs: when noise randomly increases calcium leaving the ER (negative term in first equation), it simultaneously increases calcium entering the cytosol (positive term in second equation), preserving conservation of calcium.

2.3.2 Multiplicative Noise

Multiplicative noise captures state-dependent fluctuations where the noise amplitude scales proportionally with the underlying process. This occurs when the number of active channels fluctuates randomly around some mean value—when many channels are conducting (large flux), the absolute fluctuation magnitude is larger than when few channels are conducting (small flux):

$$dX_t = f(X_t, t)dt + \sigma_{\mathrm{mult}}|J_{\mathrm{ER,out}}|dW_t$$

The noise strength now depends on $|J_{\mathrm{ER,out}}|$, the absolute magnitude of the calcium release flux. When calcium is rushing out of the ER during the rising phase of an oscillation, fluctuations are large. During the trough when flux is minimal, fluctuations are correspondingly small. The implementation for calcium dynamics becomes:

$$d[\mathrm{Ca}^{2+}]_{\mathrm{ER}} = \mu_M \delta_{\mathrm{ER}}(J_{\mathrm{SERCA}} - J_{\mathrm{ER,out}})dt - \sigma_{\mathrm{mult}}\mu_M \delta_{\mathrm{ER}}|J_{\mathrm{ER,out}}|dW_t$$
$$d[\mathrm{Ca}^{2+}]_c = \mu_M f_c(-J_{\mathrm{SERCA}} + J_{\mathrm{ER,out}} + \delta(J_{\mathrm{NCX}} - J_{\mathrm{uni}}))dt + \sigma_{\mathrm{mult}} f_c \delta_{\mathrm{ER}}|J_{\mathrm{ER,out}}|dW_t$$

2.3.3 State-Dependent Noise with Sublinear Scaling

A more refined model recognizes that fluctuations from discrete molecular events—individual channel openings and closings—produce noise whose variance scales sublinearly with the mean flux. This arises from the statistical physics of shot noise: when N independent channels each release calcium stochastically, the mean flux scales as N but the standard deviation of fluctuations scales as $\sqrt{N}$, not N. This motivates a square-root dependence:

$$dX_t = f(X_t, t)dt + \sigma_{\mathrm{state}}\sqrt{|J_{\mathrm{ER,out}}|}dW_t$$

This formulation predicts that noise grows more slowly than the signal as flux increases, representing a form of biological "noise compression." The calcium equations become:

$$d[\mathrm{Ca}^{2+}]_{\mathrm{ER}} = \mu_M \delta_{\mathrm{ER}}(J_{\mathrm{SERCA}} - J_{\mathrm{ER,out}})dt - \sigma_{\mathrm{state}}\mu_M \delta_{\mathrm{ER}}\sqrt{|J_{\mathrm{ER,out}}|}dW_t$$
$$d[\mathrm{Ca}^{2+}]_c = \mu_M f_c(-J_{\mathrm{SERCA}} + J_{\mathrm{ER,out}} + \delta(J_{\mathrm{NCX}} - J_{\mathrm{uni}}))dt + \sigma_{\mathrm{state}} f_c \delta_{\mathrm{ER}}\sqrt{|J_{\mathrm{ER,out}}|}dW_t$$

2.3.4 Colored Noise via Ornstein-Uhlenbeck Process

All previous noise types assumed temporal independence—the random fluctuation at each instant is completely unrelated to fluctuations at other times. However, many biological processes exhibit temporal correlations. Consider slow environmental fluctuations

in temperature or pH that persist for several seconds, or calcium-induced calcium release mechanisms where an initial stochastic opening event triggers subsequent openings through positive feedback, creating bursts of correlated activity.

Colored noise with temporal correlations is modeled through an auxiliary Ornstein-Uhlenbeck process—essentially a random variable that evolves according to its own stochastic differential equation and couples into the calcium dynamics:

$$d\eta_t = -\frac{\eta_t}{\tau}dt + \sigma_{\text{OU}}dW_t \qquad \frac{d[\text{Ca}^{2+}]_c}{dt} = (\ldots) + k_{\text{OU}}\eta_t \qquad \frac{d[\text{Ca}^{2+}]_{\text{ER}}}{dt} = (\ldots) - k_{\text{OU}}\eta_t$$

The variable η_t represents a random forcing that decays exponentially with time constant $\tau = 5$ seconds while being continuously perturbed by white noise. This creates a colored noise process with correlation time τ—fluctuations separated by less than τ are correlated, while those separated by much more than τ are independent. With $\tau = 5$ seconds and oscillation periods of approximately 100 seconds, this explores whether noise correlations at $\sim$5% of the oscillation period can resonate with system dynamics.

2.3.5 Jump Process Noise

Continuous diffusive noise models gradual random walks, but some biological events are discrete and intermittent. Consider spatially localized calcium puffs—abrupt, large-amplitude release events when a cluster of IP3 receptors suddenly opens in a coordinated fashion due to local calcium-induced calcium release, then rapidly inactivates. Or consider discrete vesicle fusion events in nearby neurons that release glutamate in bursts, triggering IP3 production in astrocytes. These phenomena are better captured by jump processes:

$$dX_t = f(X_t, t)dt + \sigma_{\text{jump}}dN_t$$

Here N_t is a Poisson process—a counting process that increases by 1 at random times with average rate $\lambda_{\text{jump}} = 0.01$ per second, meaning on average one jump every 100 seconds. Each jump instantly increases or decreases calcium concentrations by $\sigma_{\text{jump}} = 10^{-4}$ μM. This represents infrequent, impulsive perturbations rather than continuous diffusion.

3 Experimental Results and Analysis

3.1 Computational Implementation

The experiments employ an extended system of 30 coupled ordinary differential equations implemented in Julia, a high-performance programming language optimized for scientific computing [1]. The stochastic differential equations corresponding to additive, multiplicative, and state-dependent noise were solved using a specialized implicit Runge-Kutta-Milstein numerical method with adaptive time-stepping to ensure numerical accuracy while maintaining computational efficiency. This adaptive approach automatically reduces the time step during rapid transients (such as the rising phase of calcium oscillations) while using larger steps during slower phases, balancing accuracy against computational cost.

[1] Github: `https://github.com/bingyulab/SPDE`

Colored noise simulations employed the ISSEM (Implicit Split-Step Exponential Method), which treats the deterministic and stochastic components separately to improve numerical stability for processes with temporal correlations. Jump processes were implemented using Gillespie's direct method, an exact stochastic simulation algorithm that generates random jump times from the Poisson process while preserving the correct statistical distribution.

Each simulation ran for 4000 seconds, with the first 3000 seconds discarded as transient behavior to ensure the system reached its steady-state oscillatory regime. Only the final 1000 seconds were analyzed, capturing approximately 10 complete oscillation cycles. Critically, different random number generator seeds were used for each noise type, ensuring that the random fluctuations are genuinely independent realizations rather than the same noise sequence applied in different ways.

4 Results

4.1 Verification

Before examining metabolic robustness, we must first verify that the five noise implementations actually produce different calcium dynamics—otherwise, any observed similarity in downstream metabolism would be trivial. To quantify trajectory differences, we computed pairwise correlations between ER calcium time series and calculated mean absolute errors (MAE) and maximum differences.

Table 1 presents results for selected pairs from the 15 possible comparisons (5 noise types choosing 2). The most striking finding is that negative correlations emerge between certain pairs: additive versus colored noise shows correlation of -0.560, meaning when one noise type drives ER calcium upward, the other tends to drive it downward. This anti-phase relationship indicates fundamentally different dynamical responses, not merely quantitative variations. Other pairs show weak positive correlations (multiplicative versus state-dependent: $+0.337$), indicating partial synchrony but substantial differences.

Table 1: ER Calcium Trajectory Correlations Between Noise Types (Representative Pairs from 15 Total Comparisons)

Comparison	**Correlation**	**MAE (μM)**	**Max Diff (μM)**	**Status**
Additive vs. Colored	-0.560	7.53	12.44	Different
Multiplicative vs. Colored	-0.663	7.81	12.52	Different
Colored vs. Jump	-0.734	8.09	12.48	Different
Additive vs. Jump	$+0.539$	3.32	11.15	Different
Multiplicative vs. State-dep.	$+0.337$	3.75	12.52	Different

The large mean absolute errors (3-8 μM) are biologically significant—typical ER calcium concentrations range from 200-500 μM in the model, so these differences represent 1-4% deviations sustained over time.

4.2 Cytosolic Calcium Comparison

Having established that ER calcium dynamics differ substantially across noise types, we now examine whether these differences propagate to the cytosol—the main cellular com-

partment where calcium triggers metabolic responses. Figure 4 displays six key metabolic variables under all noise conditions, revealing a striking pattern: despite genuinely different ER dynamics, cytosolic calcium maintains remarkably consistent oscillatory behavior.

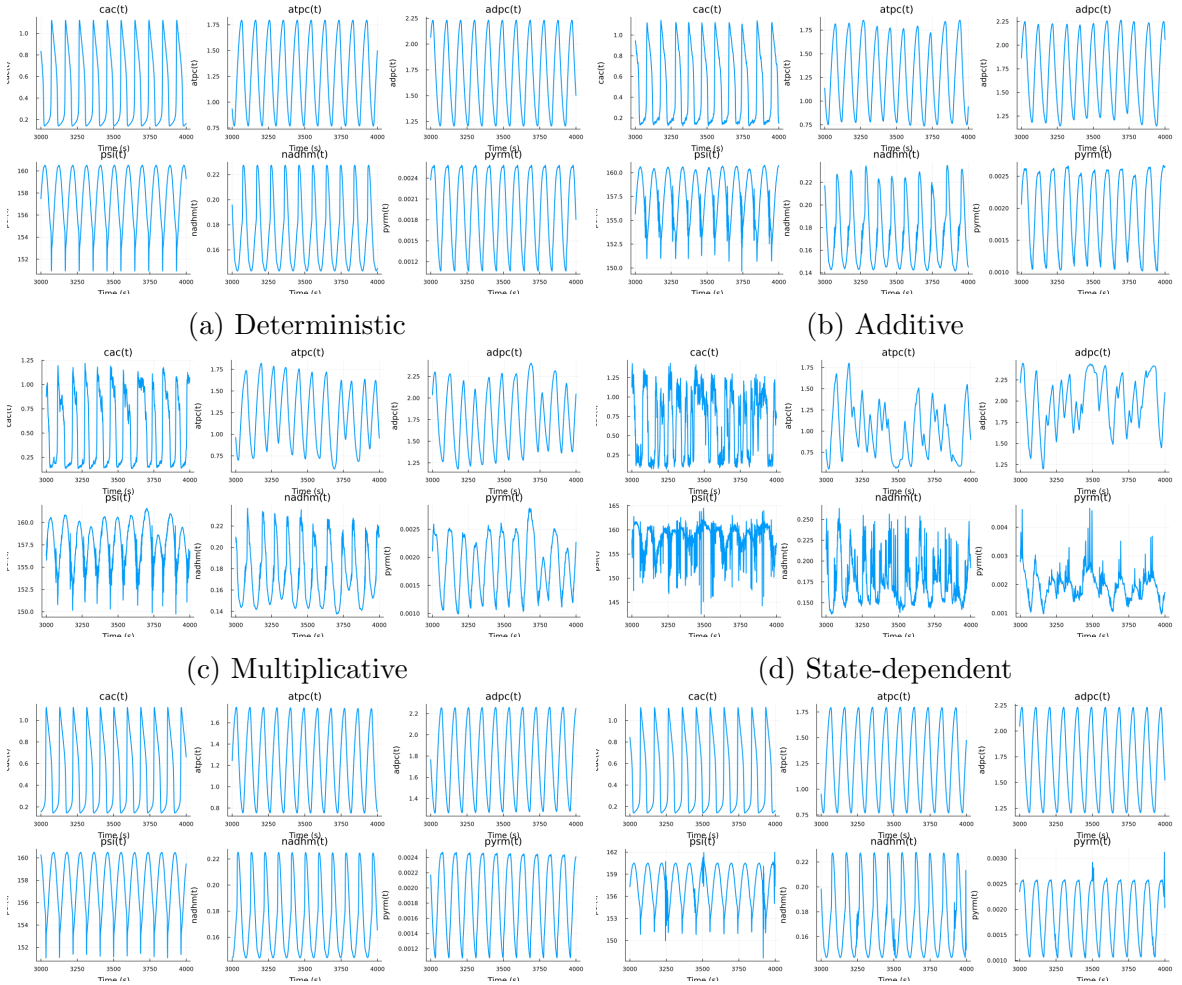

(a) Deterministic (b) Additive

(c) Multiplicative (d) State-dependent

(e) Colored (f) Jump

Figure 4: Six key metabolic variables under different noise implementations. Each panel shows time evolution of cytosolic calcium (CaC), cytosolic ATP (ATP_c), cytosolic ADP (ADP_c), mitochondrial membrane potential (PSI), mitochondrial NADH ($NADH_m$), and mitochondrial pyruvate ($Pyruvate_m$).

Table 2 quantifies this robustness through mean and standard deviation statistics. All noise types except state-dependent produce cytosolic calcium oscillations centered around 0.5 mM (millimolar concentration), with standard deviations of approximately 0.36 mM. The coefficient of variation—standard deviation divided by mean—remains consistently around 65-75%, indicating that the oscillation amplitude relative to the baseline is preserved across noise conditions.

Table 2: Cytosolic Calcium Statistical Summary Across Noise Types

Statistic	None	Additive	Multiplicative	State-dependent	Colored	Jump
Mean (mM)	0.548	0.499	0.527	0.667	0.514	0.487
Std Dev (mM)	0.362	0.356	0.371	0.419	0.354	0.355

State-dependent noise produces a notably elevated baseline (0.667 mM) and increased standard deviation (0.419 mM), foreshadowing its unique disruptive effects that will become more apparent in metabolic outputs. The square-root scaling $\sqrt{|J_{\text{ER,out}}|}$ creates a nonlinear interaction between noise amplitude and system state that differs fundamentally from the other noise types.

4.3 ATP:ADP Ratio

The most remarkable finding emerges when examining the ATP:ADP ratio—the key indicator of cellular energetic state (Figure 5). ATP and ADP (adenosine di-phosphate, the "spent" form after ATP releases energy) exist in a dynamic equilibrium maintained by metabolic processes. The ratio between them determines the thermodynamic driving force for all ATP-consuming cellular reactions, making it a critical functional output.

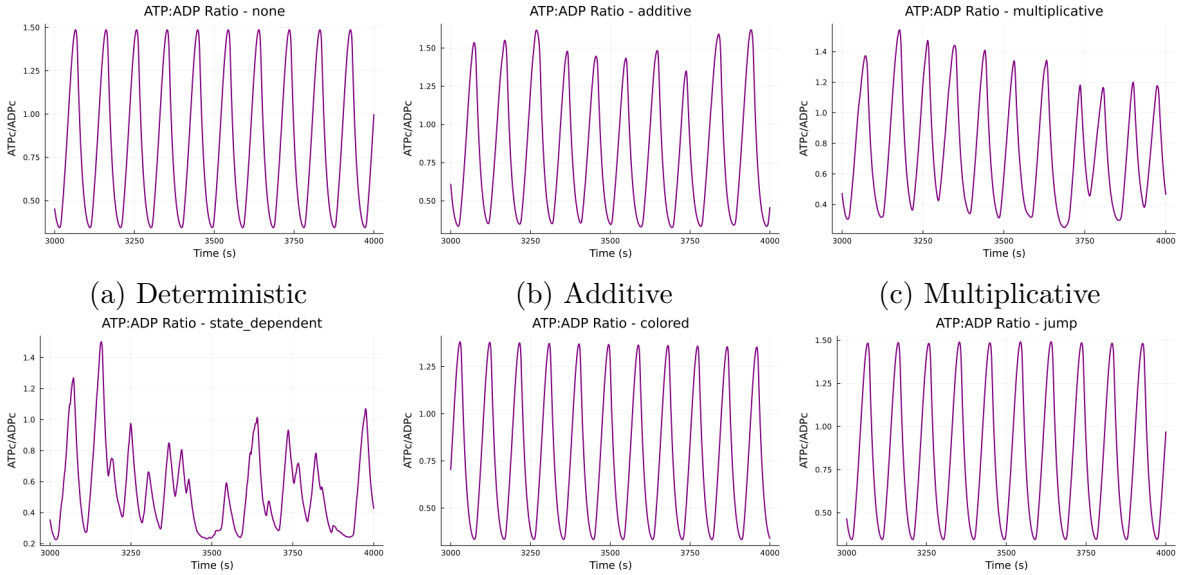

(a) Deterministic (b) Additive (c) Multiplicative

(d) State-dependent (e) Colored (f) Jump

Figure 5: ATP:ADP ratio time evolution.

The deterministic case (panel a) shows perfectly regular oscillations cycling from 0.3 to 1.6 and back with a period of approximately 100 seconds. Remarkably, additive, multiplicative, colored, and jump noise (panels b, c, e, f) all produce virtually indistinguishable traces, despite the dramatically different ER calcium dynamics underlying them. This represents complete noise filtering: stochastic perturbations that substantially alter ER dynamics have essentially zero effect on the metabolic output. State-dependent noise again stands as the exception (panel d). The ATP:ADP ratio shows irregular oscillations with amplitude modulation—the oscillation amplitude itself varies over time, creating a beating pattern.

4.4 Calcium-ATP Phase Relationships

To understand how calcium signals translate into metabolic responses, Figure 6 overlays cytosolic calcium and ATP time courses, revealing their temporal relationship.

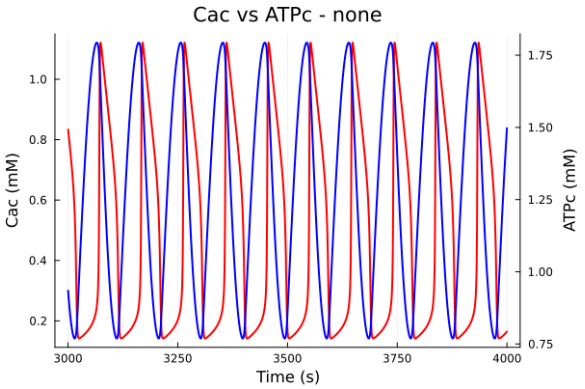

(a) Deterministic: Perfect Phase Lock

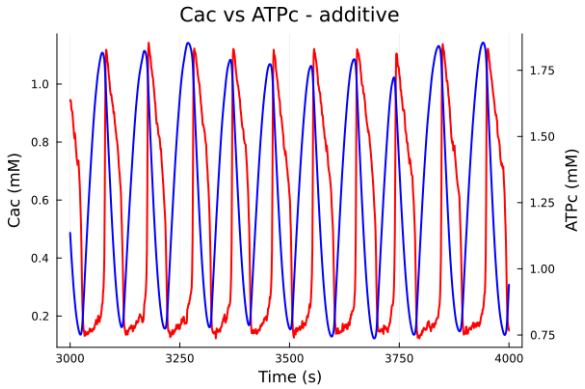

(b) Additive: Preserved Phase Lag

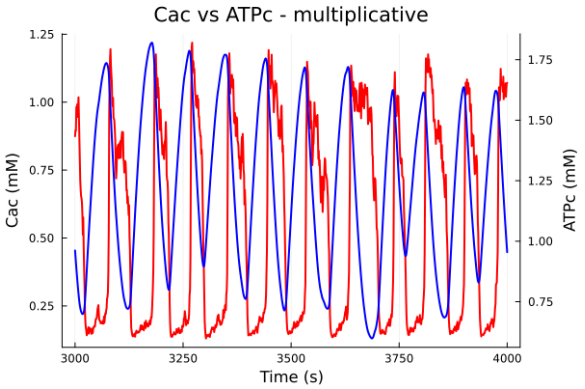

(c) Multiplicative: Phase Lock with Jitter

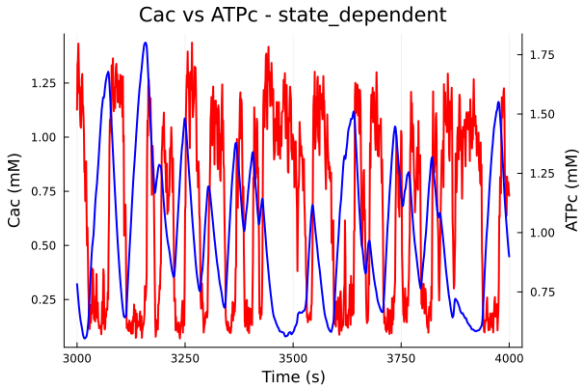

(d) State-dependent: Irregular Coupling

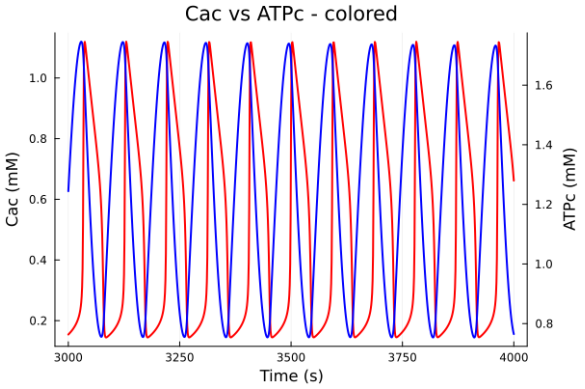

(e) Colored: Tight Phase Lock

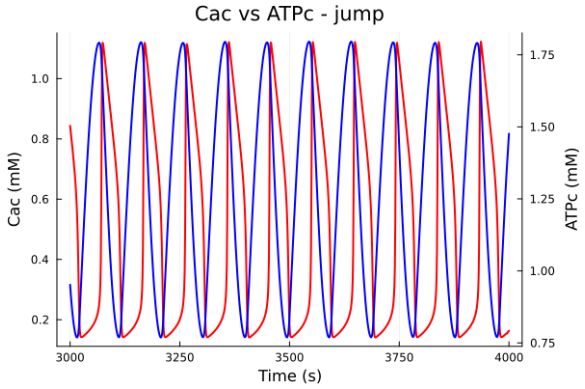

(f) Jump: Regular with Transients

Figure 6: Overlaid time courses of cytosolic calcium (blue, left axis) and ATP (red, right axis) reveal preserved phase relationships under most noise conditions. ATP peaks consistently lag calcium peaks by approximately 10 seconds in deterministic, additive, multiplicative, colored, and jump cases, reflecting the metabolic delay between calcium signal and mitochondrial ATP production. State-dependent noise disrupts this regularity, producing erratic ATP dynamics and loss of phase coherence.

The deterministic case (panel a) shows perfect phase locking: each calcium peak is followed approximately 10 seconds later by an ATP peak. T

Additive, multiplicative, colored, and jump noise (panels b, c, e, f) all preserve this phase relationship despite adding visible jitter to both calcium and ATP traces. The system maintains temporal coordination even when individual peak heights fluctuate. This suggests the existence of a robust limit cycle attractor in the coupled calcium-

metabolic phase space that resists perturbations by attracting nearby trajectories back to the nominal oscillatory path.

State-dependent noise again produces the most dramatic disruption (panel d). The ATP trace shows high-frequency fluctuations superimposed on irregular low-frequency envelope modulation. The phase relationship becomes erratic, with some calcium peaks producing robust ATP responses while others produce weak or delayed responses. This loss of phase coherence indicates that state-dependent noise can kick the system between different dynamical regimes rather than merely adding fluctuations around a stable trajectory.

5 Conclusions

This investigation reveals a hierarchical robustness architecture in astrocyte calcium-metabolic coupling, with different cellular compartments providing distinct levels of noise filtering. The findings challenge the notion that biological systems are uniformly robust to all forms of stochasticity while revealing which noise characteristics pose the greatest challenges to cellular homeostasis.

References

[1] Pellerin L, Magistretti PJ. Glutamate uptake into astrocytes stimulates aerobic glycolysis: a mechanism coupling neuronal activity to glucose utilization. *Proc Natl Acad Sci USA*. 1994;91(22):10625-9.

[2] Magistretti PJ. Neuron-glia metabolic coupling and plasticity. *J Exp Biol*. 2006;209:2304-11.

[3] Foskett JK, White C, Cheung KH, Mak DD. Inositol trisphosphate receptor Ca^{2+} release channels. *Physiol Rev*. 2007;87(2):593-658.

[4] Voorsluijs V, Avanzini F, Falasco G, Esposito M, Skupin A. Calcium oscillations optimize the energetic efficiency of mitochondrial metabolism. *iScience*. 2024;27:109078.